Supplemental Figures and their Legends

A novel pathway combining calreticulin exposure and ATP secretion in immunogenic cancer cell death

Abhishek D. Garg, Dmitri V. Krysko, Tom Verfaillie, Agnieszka Kaczmarek, Gabriela B. Ferreira, Thierry Marysael, Noemi Rubio, Malgorzata Firczuk, Christine Michiels, Chantal Mathieu, Anton J. M. Roebroek, Wim Annaert, Jakub Golab, Peter de Witte, Peter Vandenabeele and Patrizia Agostinis

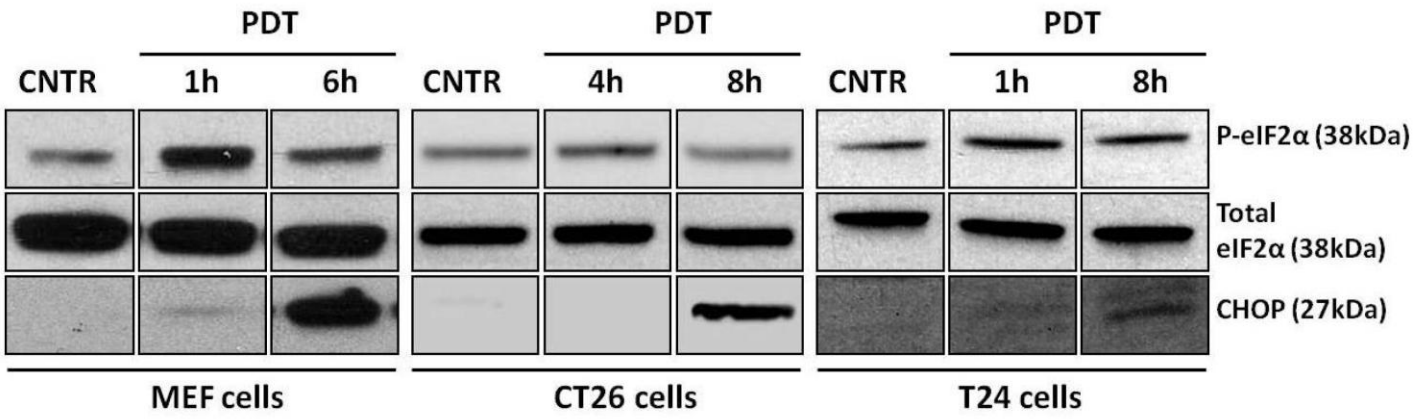

Figure S1. Hyp-PDT induces ER stress. MEFs, CT26 and T24 cells were treated with a medium PDT dose (1.35 J/cm^2, 5 min) or left untreated (CNTR). Whole-cell lysates were electrophoresed and immunoblotted for the relevant proteins at the indicated times after PDT.

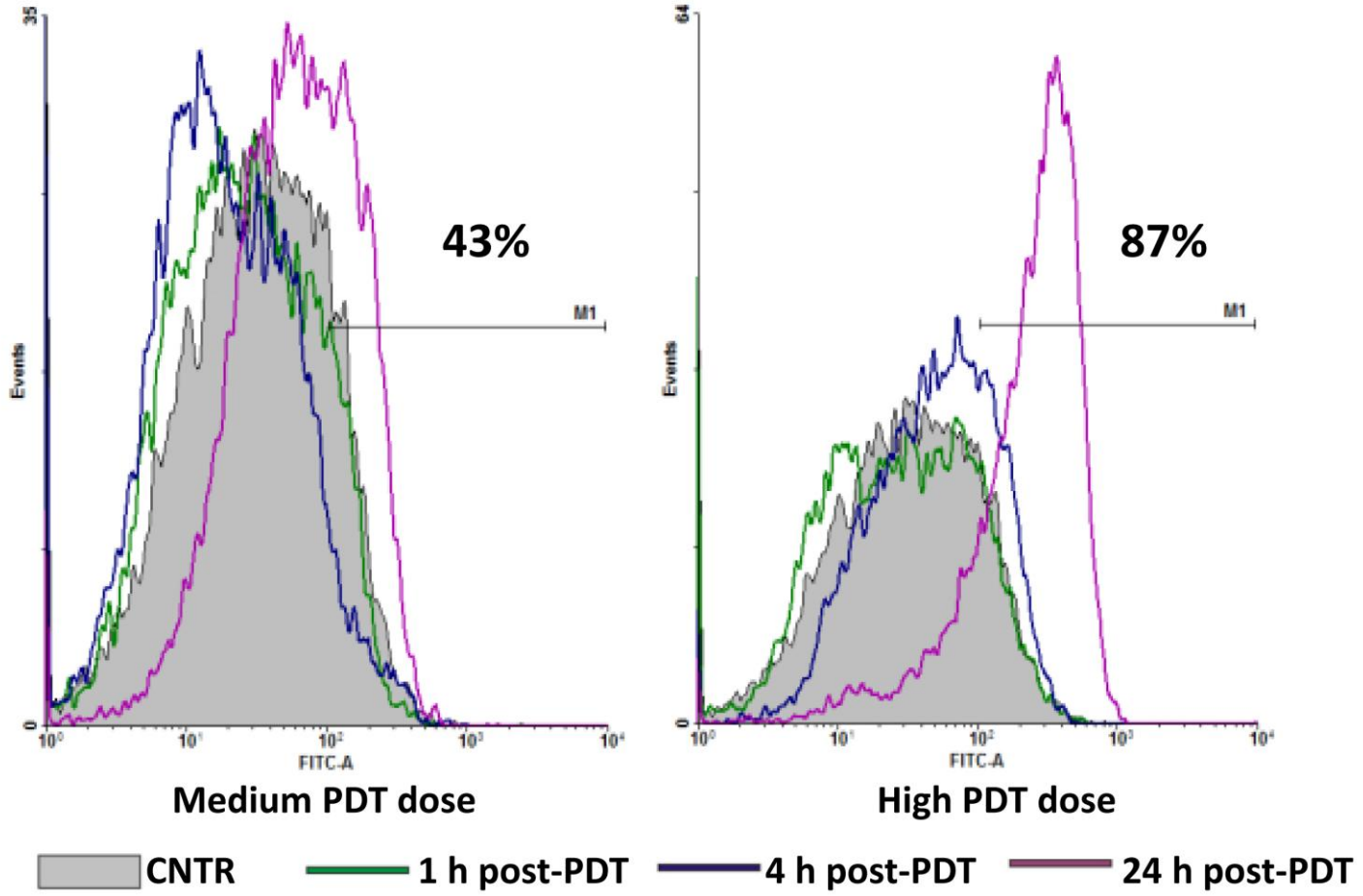

Figure S2. Phox-ER stress induces cell death, estimated *via* kinetics of phosphatidylserine (PS) exposure. T24 cells were treated with the indicated doses of PDT and recovered at three time-points after treatment, *i.e.* 1 h (green), 4 h (blue) and 24 h (magenta). Untreated T24 cells served as controls (CNTR) and are represented as a solid grey peak. The cells were then stained with annexin V–FITC and scored with FACS analysis. The representative percentage values of Annexin-V positive cells after 24 h are given above the bar (for three determinations).

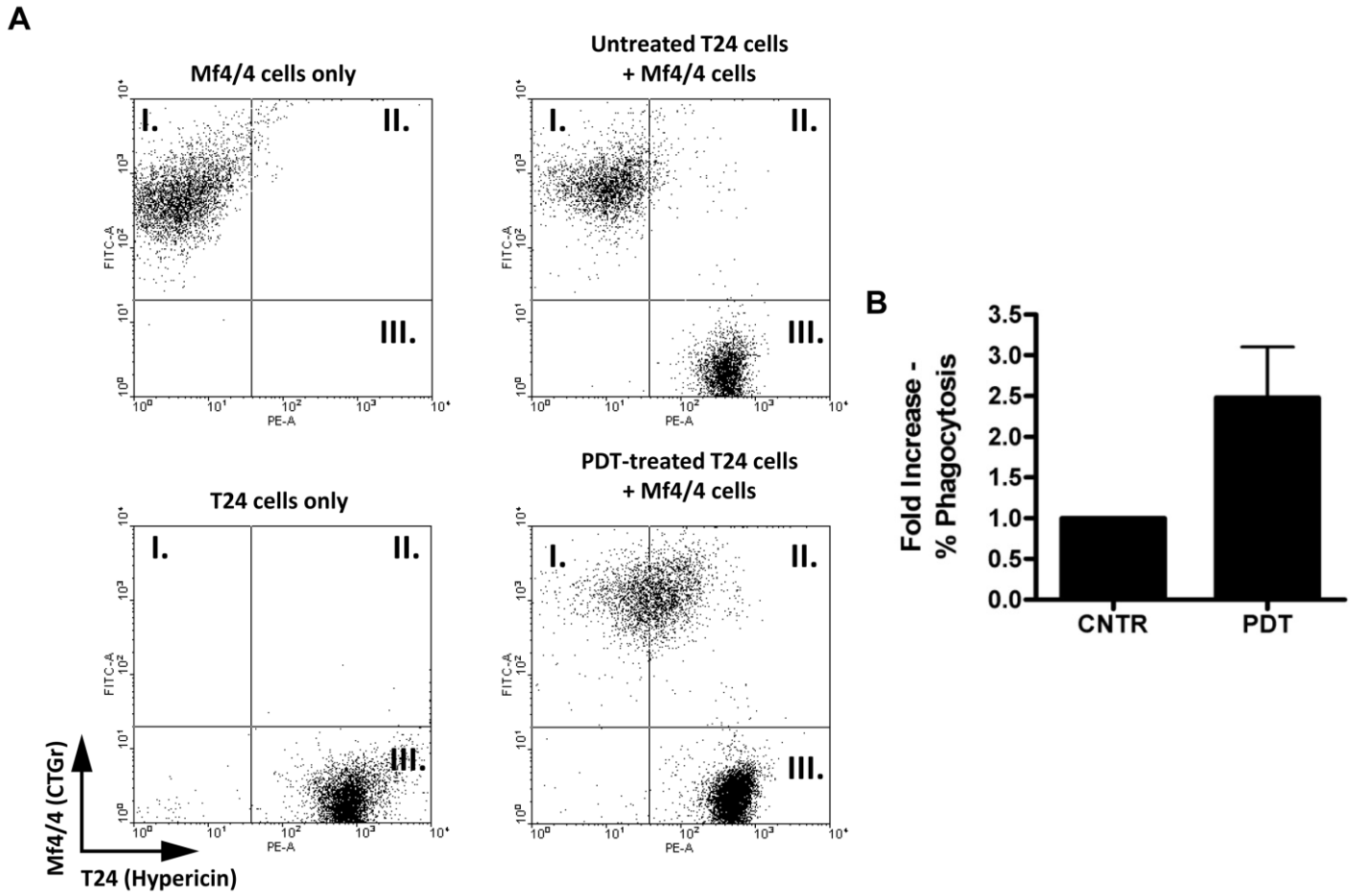

Figure S3. Phox-ER stressed cancer cells are efficiently phagocytosed by Mf4/4 phagocytes. Hypericin-labelled T24 cells were either left untreated (CNTR) or treated with a high PDT dose. They were then co-incubated with Cell Tracker Green (CTGr)-labelled Mf4/4 cells followed by FACS-based analysis of phagocytosis. Representative pictograms have been shown (A) along with the calculated fold change in % phagocytosis (B). Mf4/4 cells accumulated in quadrant I (no phagocytosis) and quadrant II (phagocytic uptake) while free T24 cells accumulated in quadrant III. Data has been normalized to the CNTR values. Values are means of two independent experiments (two replicate determinations in each) ± SEM.

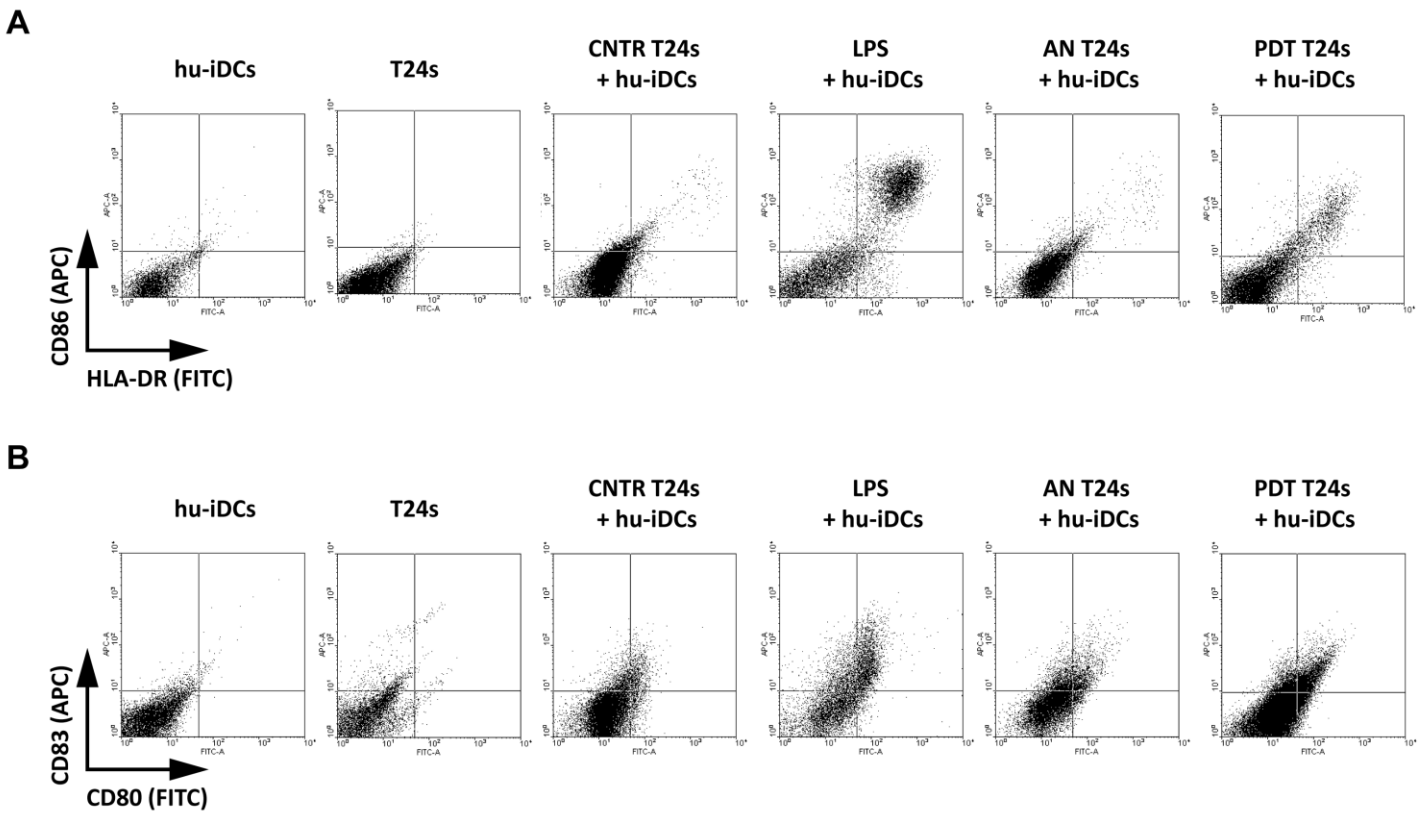

Figure S4. Phox-ER stressed cancer cells induce phenotypic maturation of DCs. T24 cells were left untreated (CNTR), treated to undergo accidental necrosis (AN), or treated with a high PDT dose (24 h post-PDT recovery time-point). They were then co-incubated with human immature dendritic cells (hu-iDCs) for 24 h. As a positive control, hu-iDCs were stimulated with LPS for 24 h. After co-incubation/stimulation, the cells were immunostained in two separate groups for CD86/HLA-DR positivity (A) and CD80/CD83 positivity (B); and scored by FACS analysis. Representative pictograms have been shown for two independent experiments with two replicate determinations in each.

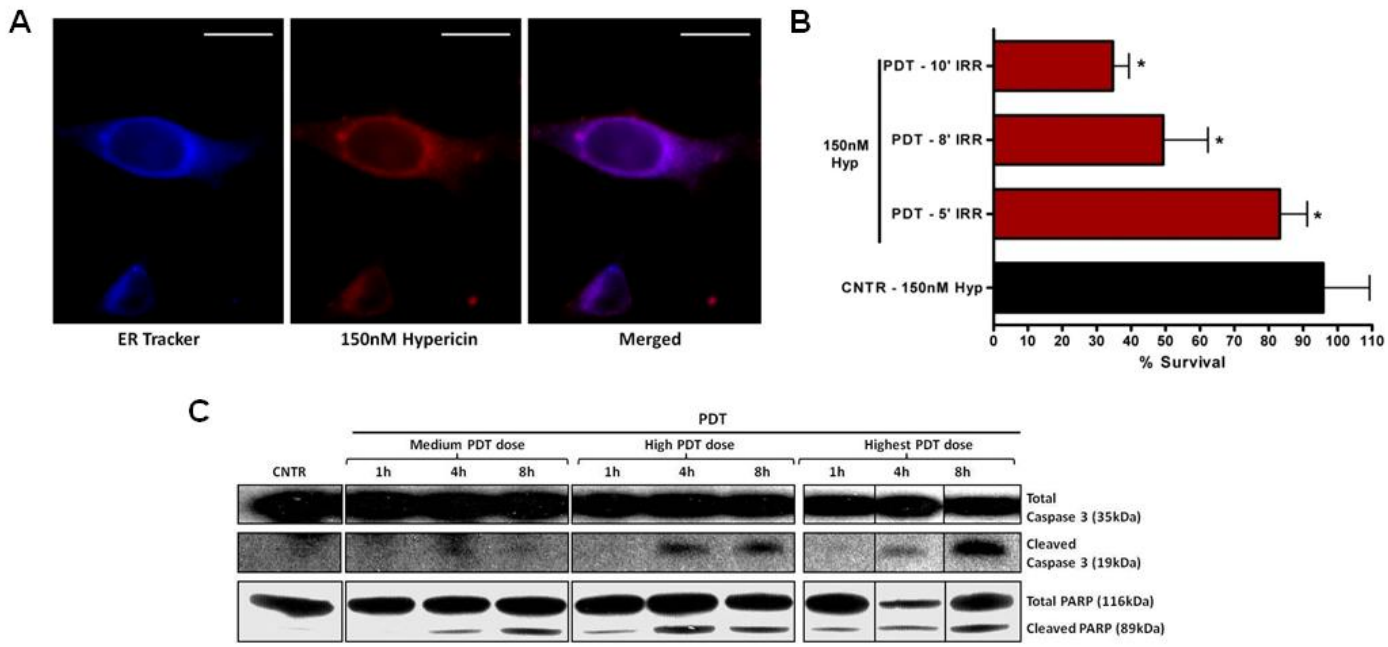

Figure S5. CT26 cells undergo apoptosis upon phox-ER stress. (A) Hypericin accumulates predominantly in the ER. CT26 cells were incubated with 150 nM Hypericin (red) for 16 h and counter-stained with ER Tracker Blue-White (Blue) so that the co-localization can be confirmed by merging fluorescence microscopy images; scale bar = 20 µm. (B) Hyp-PDT reduces CT26 viability in a light fluence-dependent manner. CT26 cells were incubated with 150 nM Hypericin for 16 h and irradiated with the suitable light wavelength: medium PDT dose, 1.35 J/cm^2, 5 min; high PDT dose, 2.16 J/cm^2, 8 min; highest PDT dose, 2.70 J/cm^2, 10 min. Cell viability was estimated with MTS assay. Data are presented as percent survival; the values are means of two independent experiments (five replicate determinations for each) ± SD (*P<0.05, vs. CNTR). (C) CT26 cells show caspase 3 and PARP cleavage after Hyp-PDT. CT26 cells were treated with the medium, high or highest PDT dose or left untreated (CNTR), and whole-cell lysates were analysed by immunoblotting.

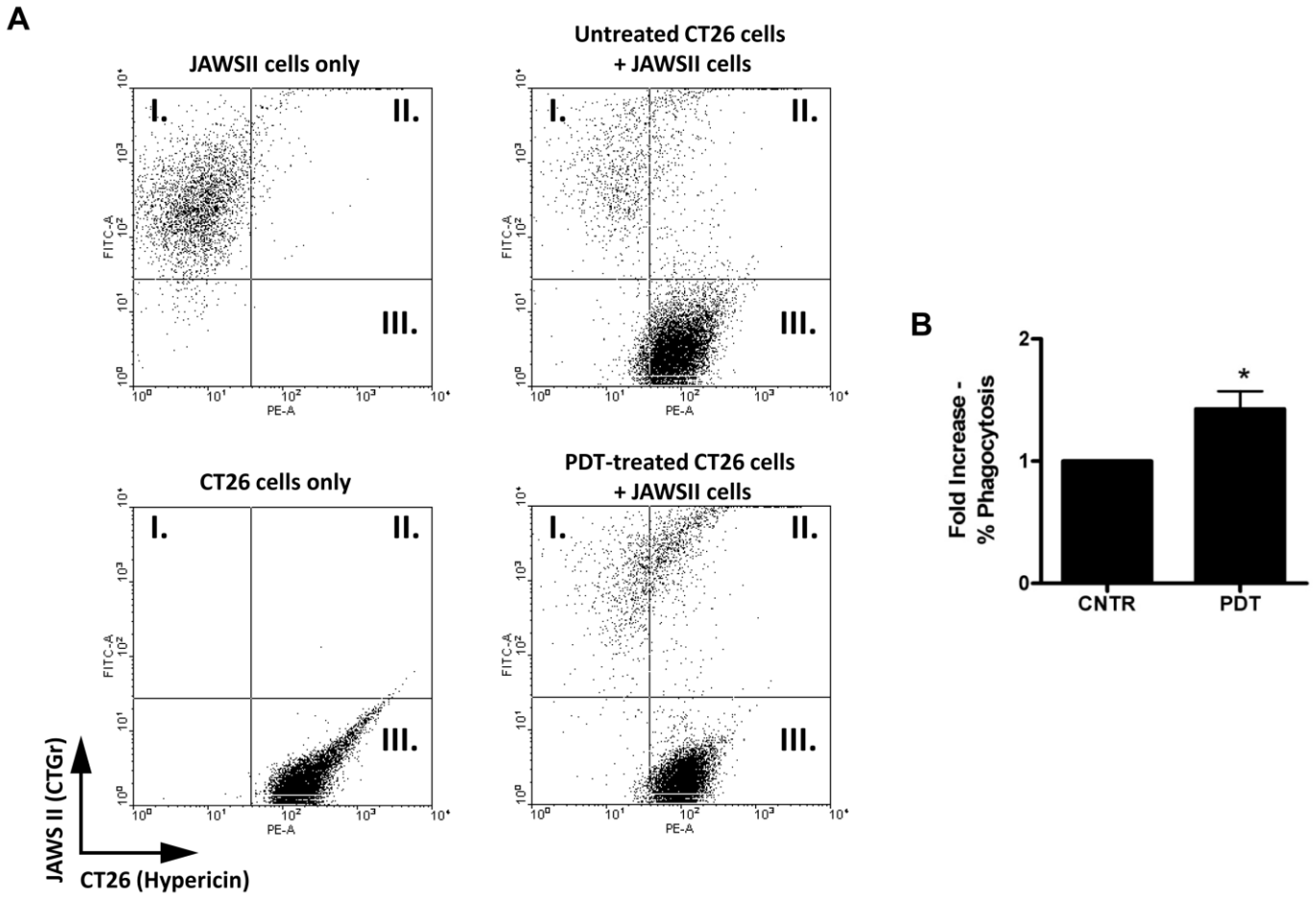

Figure S6. Phox-ER stressed cancer cells are efficiently phagocytosed by JAWSII phagocytes. Hypericin-labelled CT26 cells were either left untreated (CNTR) or treated with a high PDT dose and recovered 1 h post-PDT. They were then co-incubated with Cell Tracker Green (CTGr)-labelled JAWSII cells followed by FACS-based analysis of phagocytosis. Representative pictograms have been shown (A) along with the calculated fold change in % phagocytosis (B). JAWSII cells accumulated in quadrant I (no phagocytosis) and quadrant II (phagocytic uptake) while free CT26 cells accumulated in quadrant III. Data has been normalized to the CNTR values. Values are means of two independent experiments (two replicate determinations in each) ± SEM (*P<0.05, vs. CNTR).

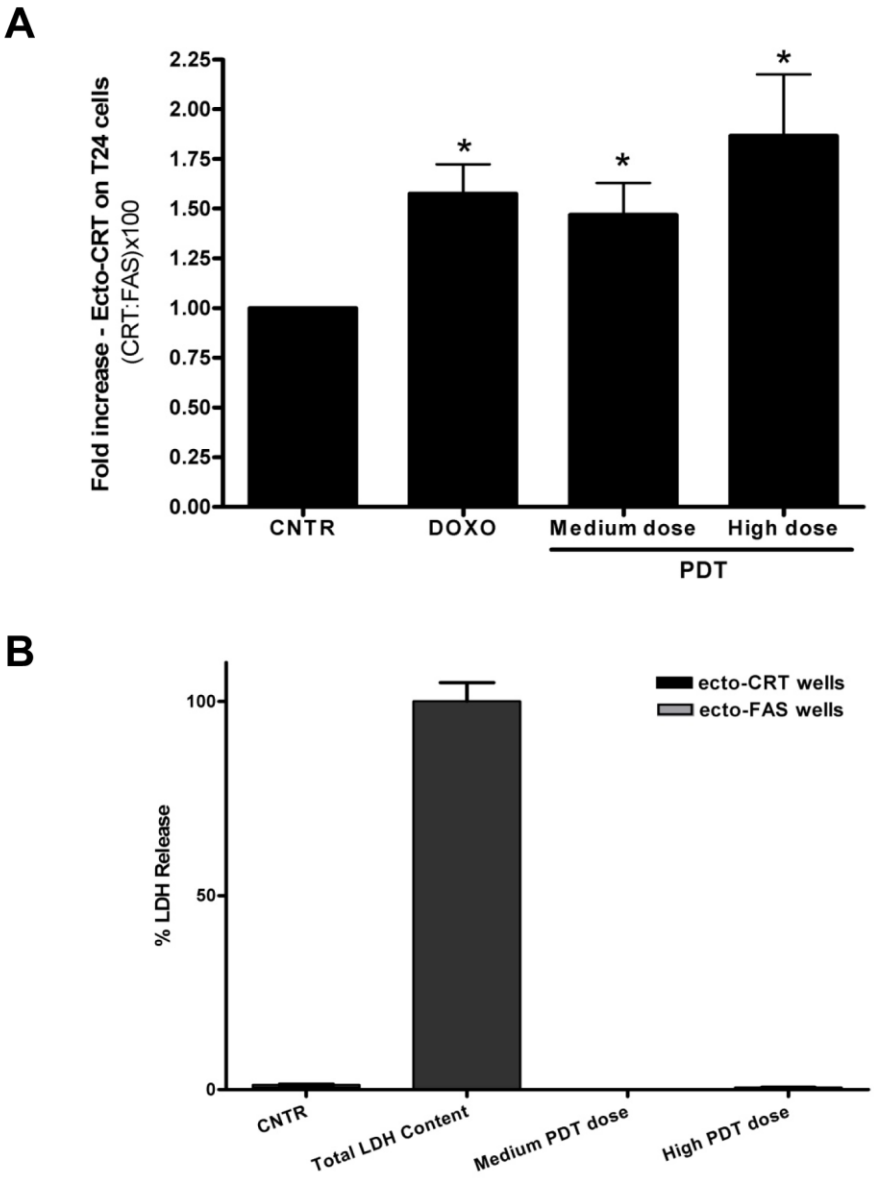

Figure S7. Phox-ER stress induces ecto-CRT in cancer cells, in the absence of plasma membrane permeabilization. T24 cells were treated with DOXO (25 μM for 4 h) or PDT (recovered 1 h post-PDT) and fixed followed by immunostaining for CRT and FAS according to the On-Cell Western protocol. The fluorescence intensity in the resulting images was quantified for the values of (A). Data are presented as fold change in the ratio of the intensities of CRT to FAS (A) relative to the CNTR samples. Simultaneously, the conditioned (serum-free) media were recuperated and the presence of cytosolic LDH was determined (B). Total LDH content was determined following Triton-based permeabilization of cells. Data are presented as percent LDH release. Values are means of triplicate determinations ±SEM (*P<0.05, vs. CNTR).

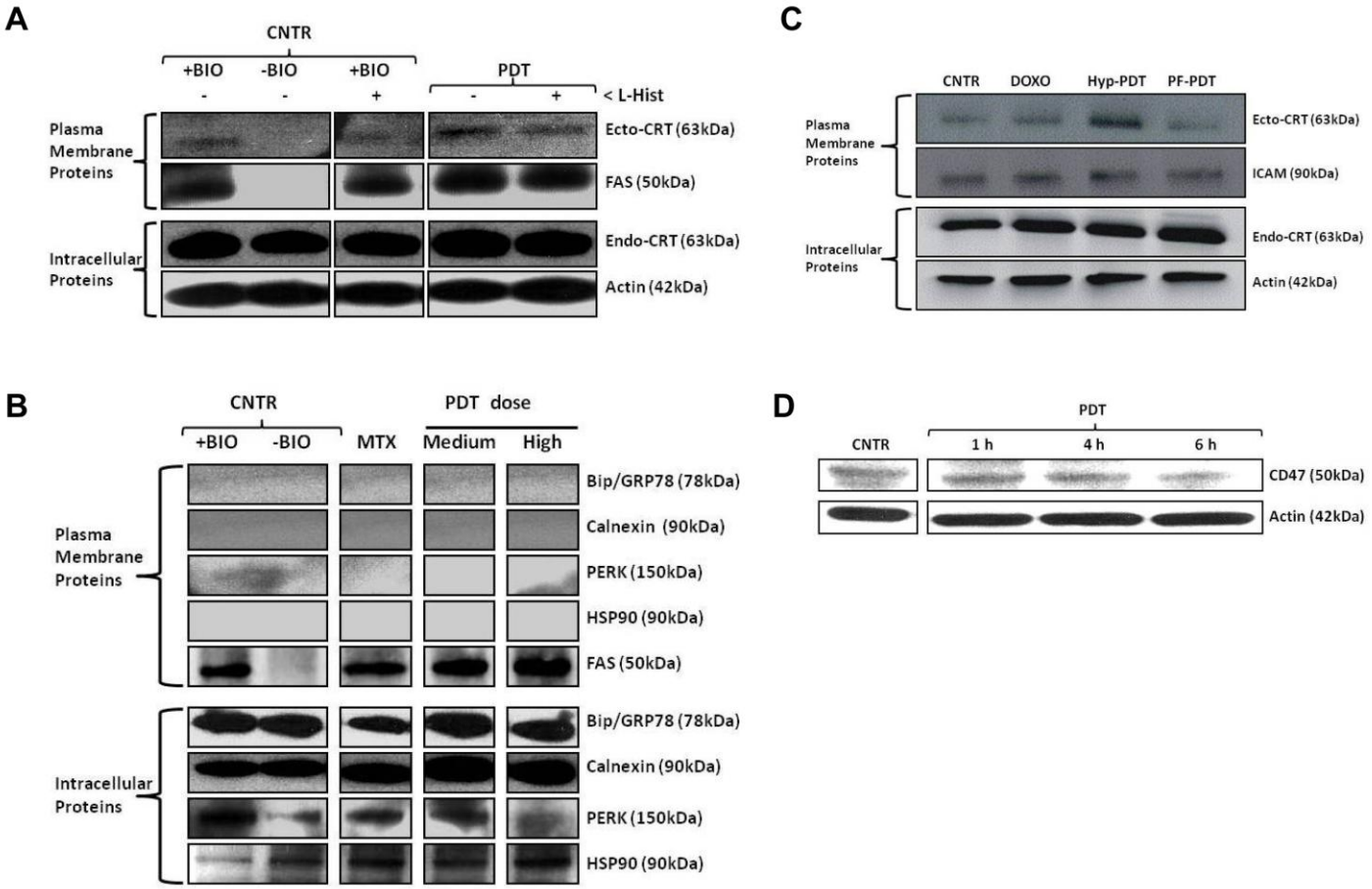

Figure S8. Hyp-PDT but not PF-PDT induces (ROS-dependent) ecto-CRT that is not accompanied by general surface scrambling of ER proteins or ecto-HSP90 exposure and precedes the decrease in CD47 levels. (A) Ecto-CRT induced by phox-ER stress is ROS-dependent. T24 cells were pre-incubated with 25 mM of L-histidine for 30 min followed by treatment with a medium PDT dose or no treatment (CNTR) and recovered 1 h post-PDT. Surface proteins were biotinylated and immunoblotted. '+BIO' indicates controls exposed to buffer with biotin and '-BIO' indicates controls exposed to buffer without biotin (negative control). (B) Phox-ER stress does not cause pre-apoptotic surface exposure of Bip/GRP78, HSP90, Calnexin and PERK. T24 cells were treated with (indicated doses of) PDT, MTX (1 μM for 4 h) or left untreated (CNTR). They were recovered 1 h post-PDT and surface biotinylation analysis was done as mentioned in A. (C) Surface biotinylation analysis for ecto-CRT, in cells treated with Hyp-PDT vs. those treated with PF-PDT. T24 cells were incubated with 300 nM hypericin for 24 h and irradiated at a fluency of 0.48 J/cm^2 for Hyp-PDT (and recovered 4 h post-PDT). Simultaneously, T24 cells were treated with Photofrin-PDT (PF-PDT, recovered after 4 h), DOXO (25 μM for 4 h) or left untreated (CNTR). Surface biotinylation analysis was done as mentioned in A. (D) CD47 levels go down after PDT treatment. T24 cells were treated with high PDT dose or left untreated (CNTR) and whole-cell lysates were prepared and immunoblotted.

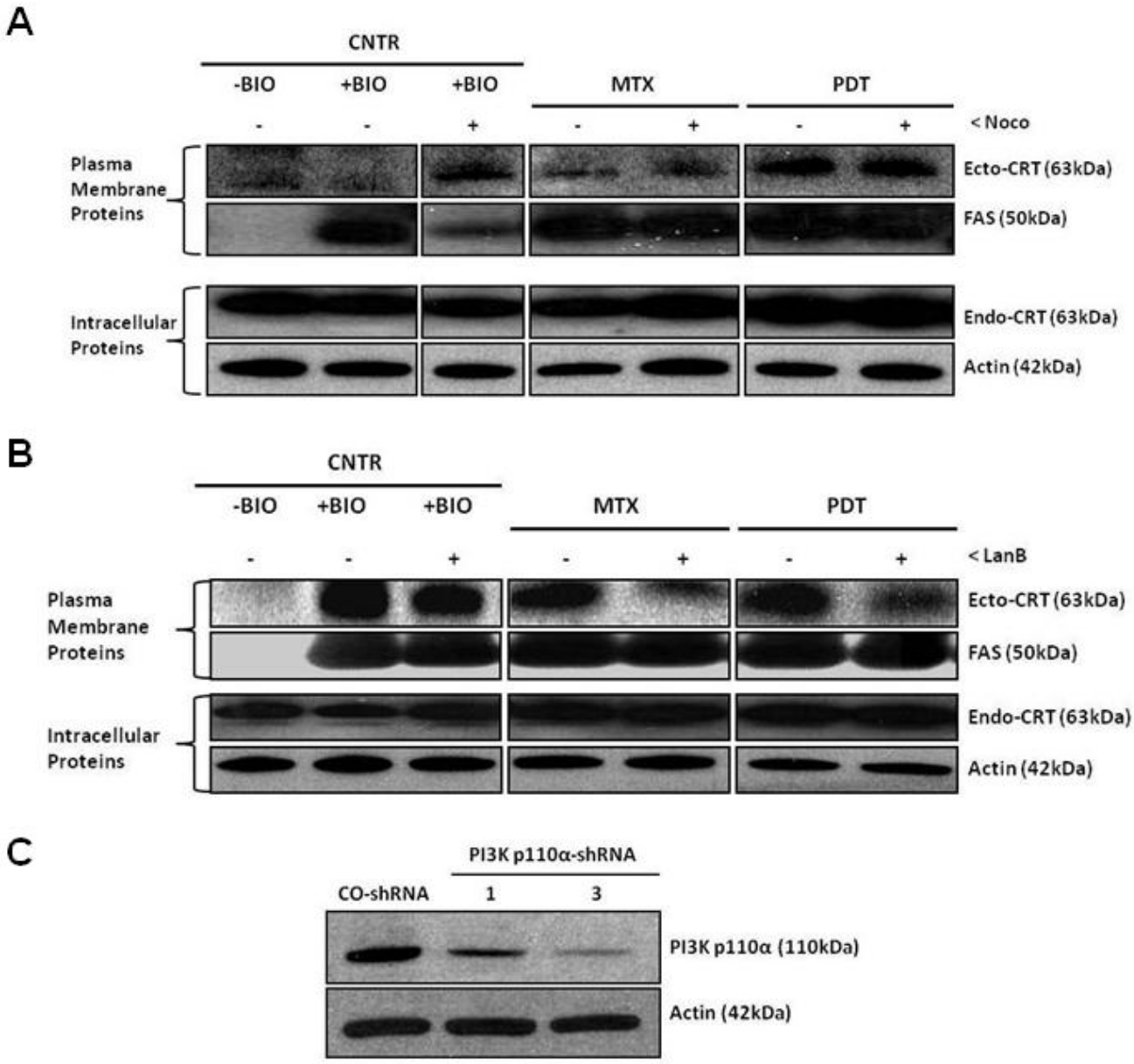

Figure S9. Phox-ER stress induced ecto-CRT is affected by latrunculin B but not nocodazole. (A and B) T24 cells were pre-incubated with either 100 nM of Nocodazole (Noco) (A) or 5 nM of Latrunculin B (LanB) (B) for 1 h followed by treatment with a medium PDT dose, MTX (1 μM for 4 h) or left untreated (CNTR), and recovered 1 h post-PDT. Surface proteins were biotinylated and immunoblotted. In A and B, '+BIO' indicates controls exposed to buffer with biotin, and '-BIO' indicates controls exposed to buffer without biotin (negative control). (C) Best knock-down of PI3K p110α is achieved *via* corresponding shRNA 3. Following stable transfection of CT26 cells with three shRNA targeted towards PI3K p110α, the knock-down was validated through immunoblotting with CO-shRNA cells used as negative control. Cells transfected with shRNA 2 did not survive selection hence could not be included in this analysis.

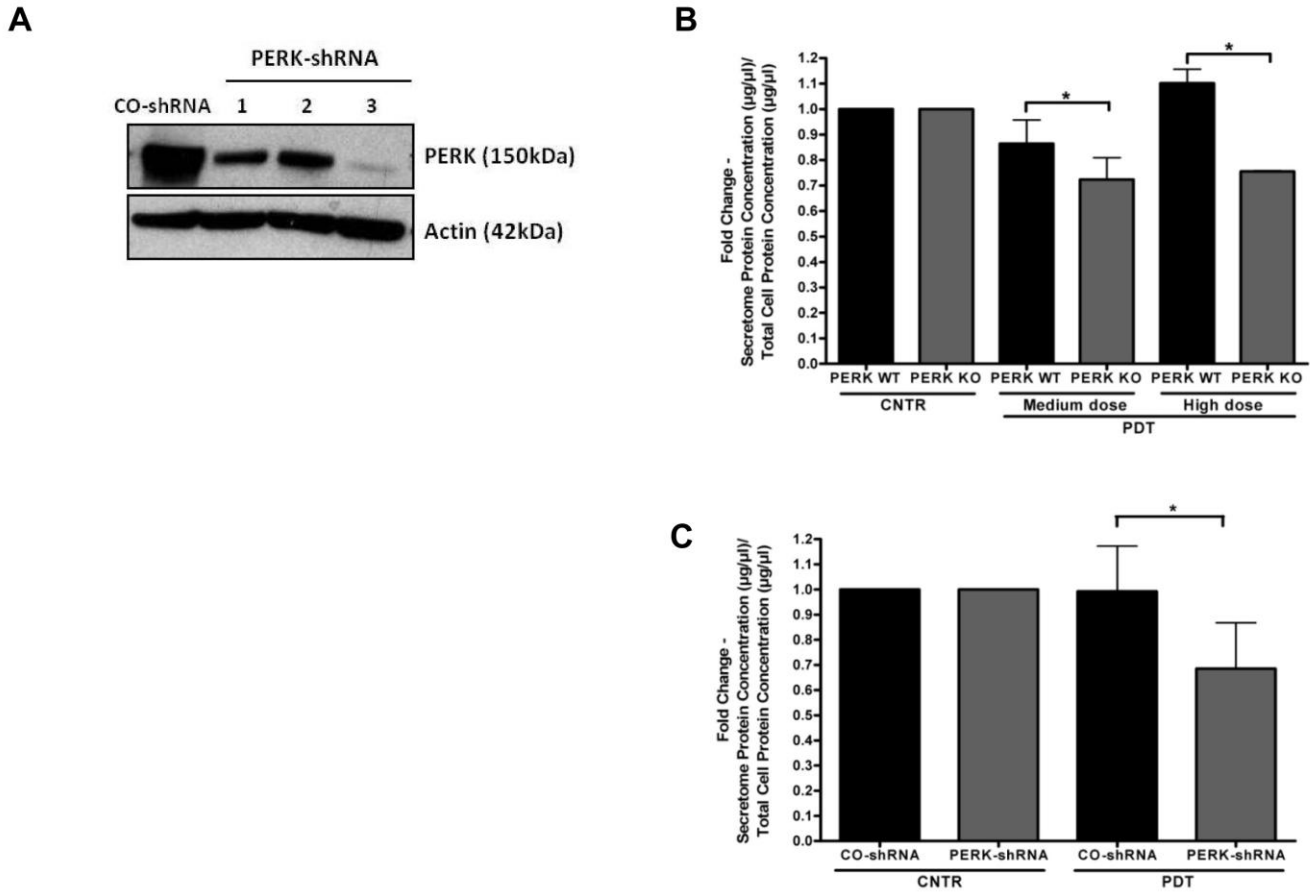

Figure S10. PERK deficient or depleted cells exhibit difficulties in maintaining/modulating total extracellular secretory protein content following phox-ER stress. (A) Best knock-down of PERK is achieved *via* corresponding shRNA 3. Following stable transfection of CT26 cells with three shRNA targeted towards PERK, the knock-down was validated through immunoblotting with CO-shRNA cells used as negative control. (B and C) PERK wild-type (WT) or knock-out (KO) MEFs were treated with indicated PDT doses (B) while CT26 cells were treated with medium PDT dose (C) or left untreated (CNTR); and both were recovered for 1 h post-PDT in serum-free media. Subsequently, the conditioned media were recuperated and concentrated followed by protein concentration estimation (secretome protein concentration). Simultaneously, whole-cell lysates were prepared for the respective cells followed by protein concentration estimation (total cell protein concentration). Data are presented as fold change in the ratio of the secretome protein concentration to total cell protein concentration relative to the CNTR samples. Values are means of three independent experiments ±SEM (*$P<0.05$).

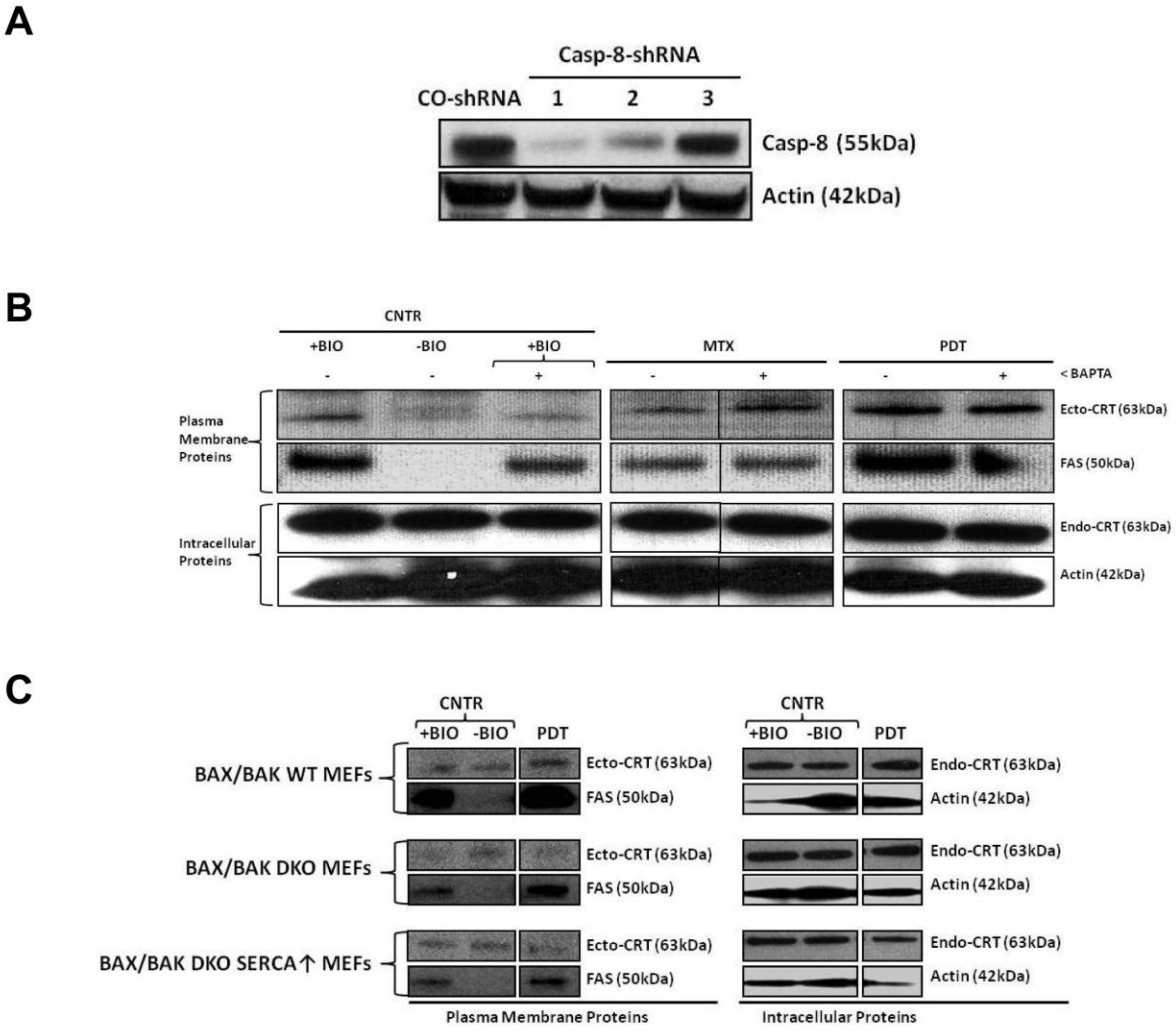

Figure S11. Induction of ecto-CRT by phox-ER stress is neither affected by cytosolic Ca^{2+} chelation nor restored after SERCA2 overexpression in cells lacking BAX/BAK. (A) Best knock-down of caspase-8 (casp-8) is achieved *via* corresponding shRNA 1. Following stable transfection of CT26 cells with three shRNA targeted towards casp-8, the knock-down was validated through immunoblotting with CO-shRNA cells used as negative control. (B) Induction of ecto-CRT by phox-ER stress is not affected due to cytosolic Ca^{2+} chelation. T24 cells were pre-incubated with 10 μM of BAPTA for 1 h and then treated with a medium PDT dose, MTX (1 μM for 4 h) or left untreated (CNTR), and then recovered 30 min later. Surface proteins were biotinylated and immunoblotted. In B and C, '+BIO' indicates controls exposed to buffer with biotin, and '-BIO' indicates controls exposed to buffer without biotin (negative control). (C) Induction of ecto-CRT by phox-ER stress is not restored by SERCA2 overexpression in cells lacking BAX/BAK. MEF cells possessing normal BAX/BAK (WT), lacking BAX/BAK (DKO), and those lacking BAX/BAK but overexpressing SERCA2 (DKO SERCA↑) were treated with a low PDT dose or left untreated (CNTR), and recovered 1 h post-PDT. This was followed by biotinylation as explained in A.

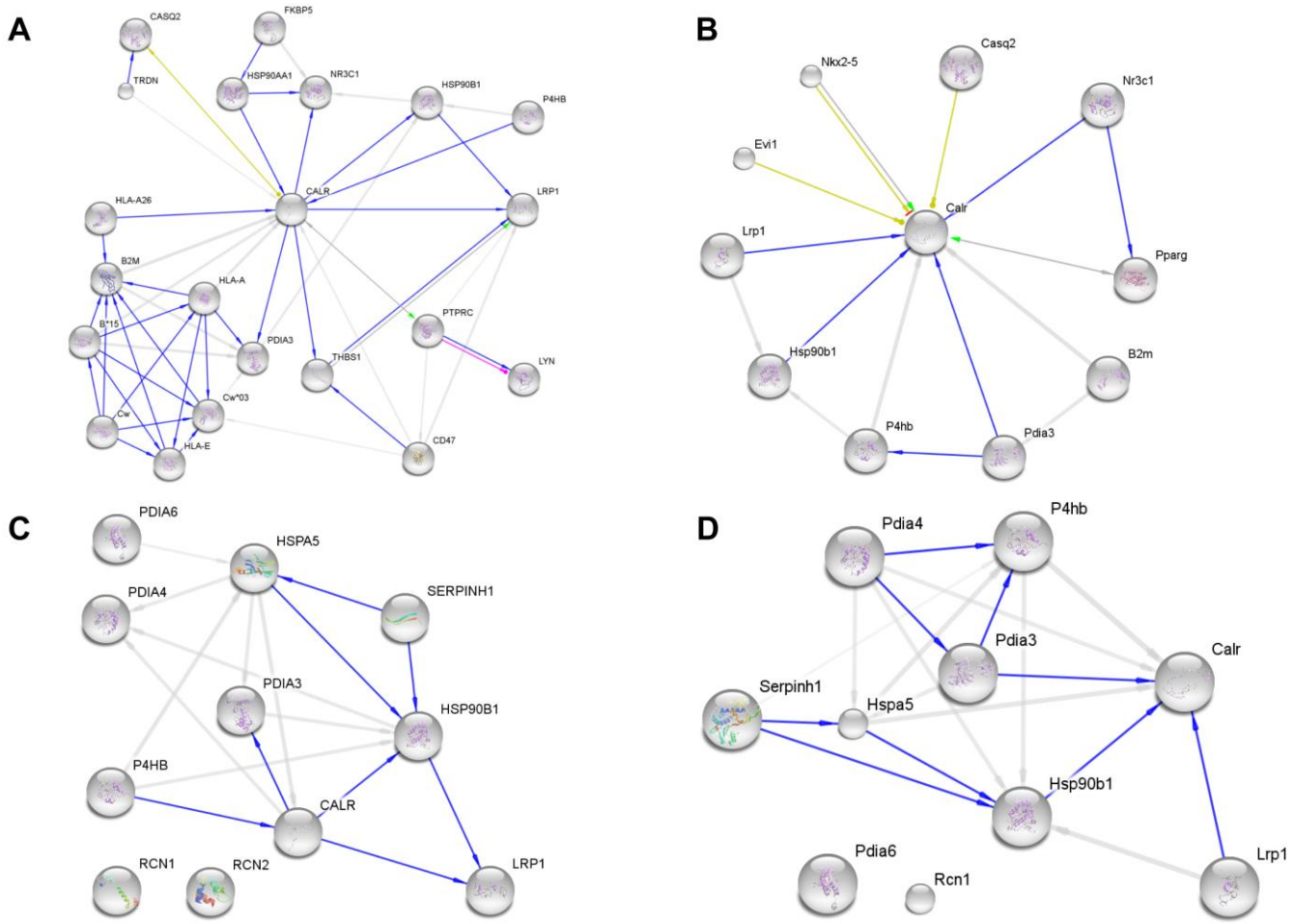

Figure S12. ***In silico*** **protein–protein binding interaction network for CRT and between LRP1 and some major proteins that possess a KDEL sequence in human and mouse.** (A and B) STRING database and web tool were used to draw binding interaction networks for CRT (denoted as CALR) in human (A) and mouse (B), with no bias towards any particular protein or interaction analysis methodology. In A, B, C and D, the blue lines indicate protein-protein binding interactions. All the proteins are indicated by the abbreviated names of the genes that encode them. (C and D) STRING database and web tool were used to cluster various major KDEL-containing proteins together and draw their binding interaction networks with LRP1 from human (C) and mouse (D), with no bias towards any particular interaction analysis methodology. The following proteins containing a KDEL sequence were used for this analysis: CALR - **CRT** (calreticulin), PDIA6 - **PDI** (protein disulfide isomerase family A, member 6), PDIA4 - **ERp72** (protein disulfide isomerase family A, member 4), PDIA3 - **ERp57** (protein disulfide isomerase family A, member 3), HSPA5 - **GRP78** (glucose-regulated protein, 78kDa or heat shock 70kDa protein 5), SERPINH1 - **HSP47** (heat shock protein 47 or serpin peptidase inhibitor, clade H), HSP90B1 - **GRP94** (glucose-regulated protein, 94kDa or heat shock protein 90kDa beta, member 1), **P4HB** (prolyl 4-hydroxylase, beta polypeptide), **RCN1** (reticulocalbin 1) and **RCN2** (Reticulocalbin-2 precursor).

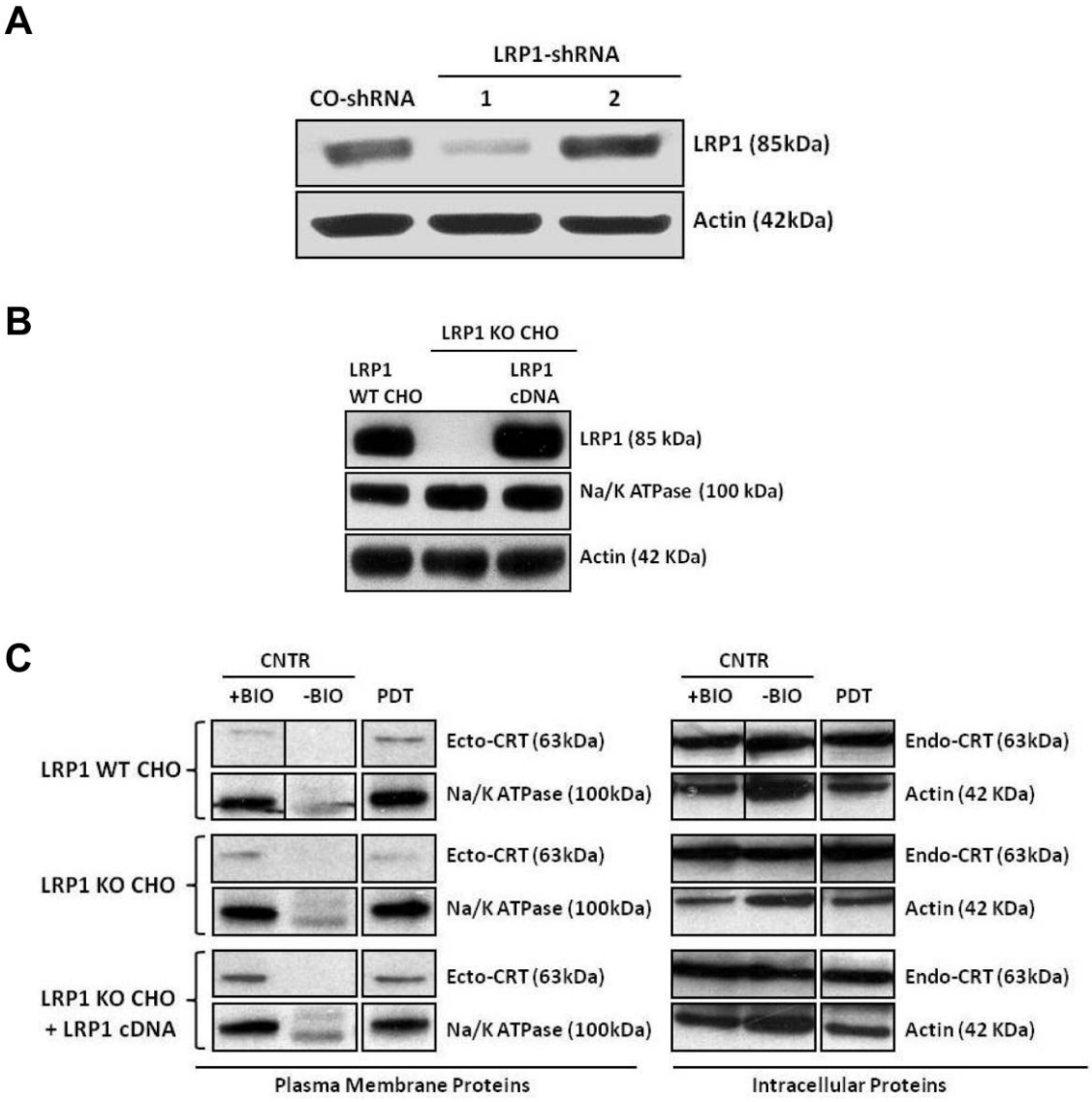

Figure S13. Cells lacking LRP1 are unable to induce ecto-CRT following phox-ER stress, which is restored following LRP1 reconstitution. (A) Best knock-down of LRP1 is achieved *via* corresponding shRNA 1. Following stable transfection of CT26 cells with three shRNA targeted towards LRP1, the knock-down was validated through immunoblotting with CO-shRNA cells used as negative control. Cells transfected with shRNA 3 did not survive selection hence could not be included in this analysis. (B) LRP1 can be successfully restored in LRP1 deficient CHO cells. LRP1 deficient (KO) Chinese hamster ovary (CHO) cells were stably transfected with a LRP1 coding cDNA thereby rescuing the original LRP1 expression noticed in LRP1 competent (WT) cells. (C) LRP1 competent (WT), deficient (KO) and reconstituted (KO + LRP1cDNA) CHO cells were treated with a low PDT dose or left untreated (CNTR), and then recovered 1 h later. Surface proteins were biotinylated and immunoblotted. '+BIO' indicates controls exposed to buffer with biotin, and '-BIO' indicates controls exposed to buffer without biotin (negative control).

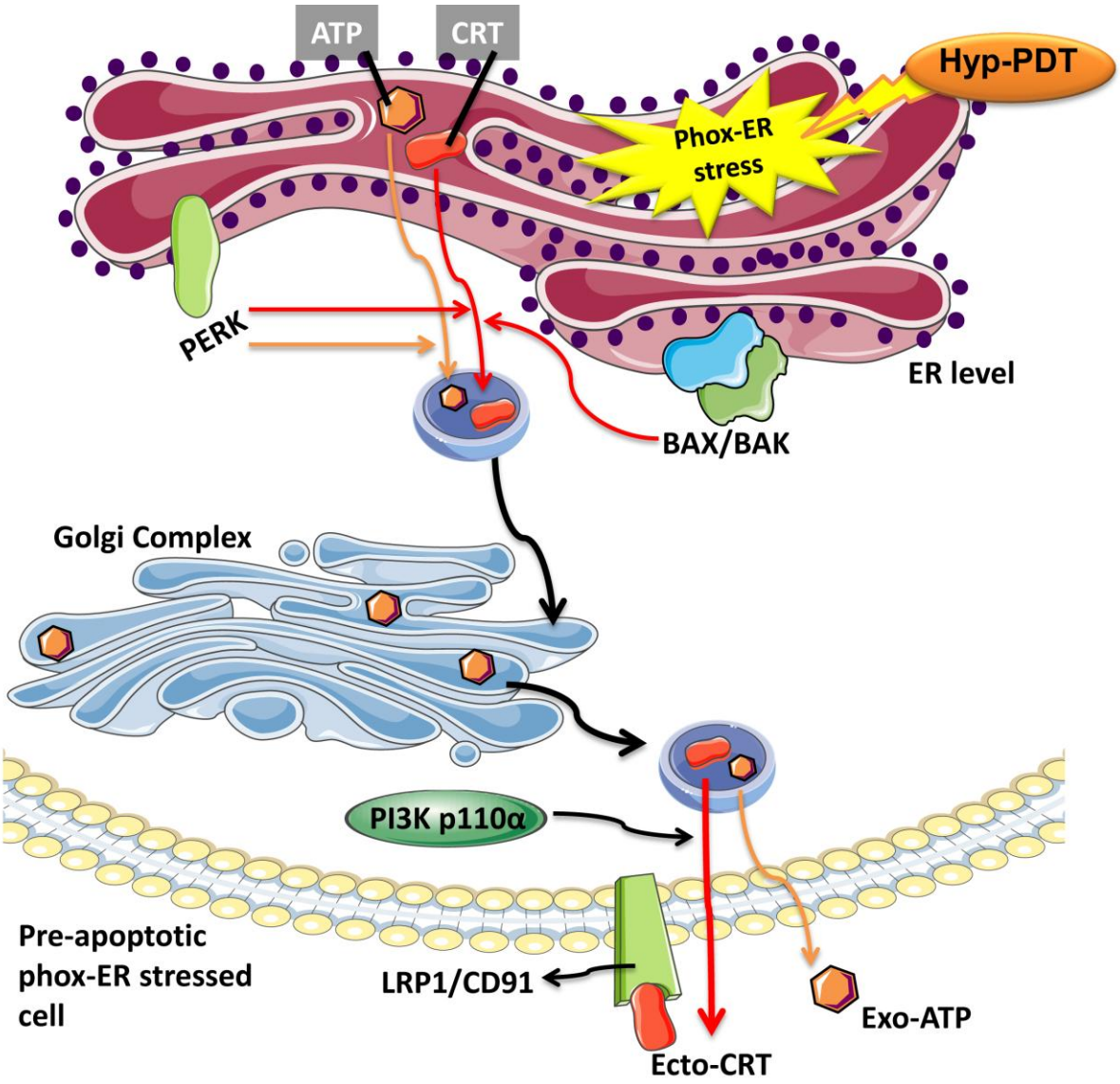

Figure S14. Hypothetical representation of the novel molecular pathway for induction of ecto-CRT and secretion of ATP induced by phox-ER stress. In response to the phox-ER stress induced by hypericin-based PDT (Hyp-PDT), CRT (but not other major ER proteins) leaves the ER before apoptosis starts *via* a pathway governed by PERK and BAX/BAK. The interactions of PERK and BAX/BAK causing this process are not yet clear although there are some indications that PERK might have some role to play in proper maintenance of extracellular secretory protein load. Beyond the ER, CRT follows the 'classical' anterograde secretory pathway and PI3K dependent vesicular exocytosis to reach the plasma membrane, where it docks on the surface *via* LRP1/CD91. Simultaneously, ATP joins CRT (either from the ER or Golgi or both) *via* a process governed by PERK but not by BAX/BAK and also follows the secretory pathway and PI3K-dependent exocytosis. Thus, following phox-ER stress but before major apoptotic changes occur; two major DAMPs conferring immunogenicity on cancer cell death are co-translocated/emitted through overlapping pathways.

Supplemental Materials and Methods

A novel pathway combining calreticulin exposure and ATP secretion in immunogenic cancer cell death

Abhishek D. Garg, Dmitri V. Krysko, Tom Verfaillie, Agnieszka Kaczmarek, Gabriela B. Ferreira, Thierry Marysael, Noemi Rubio, Malgorzata Firczuk, Christine Michiels, Chantal Mathieu, Anton J. M. Roebroek, Wim Annaert, Jakub Golab, Peter de Witte, Peter Vandenabeele and Patrizia Agostinis

Detection of plasma membrane permeabilization and analysis of cell death

Plasma membrane permeabilization was analyzed by estimating the amounts of LDH released into the serum free conditioned media using *In Vitro* Toxicology Assay Kit, LDH based (Sigma, St. Louis, MO, USA) or LDH Cytotoxicity Detection Kit (Clontech, Mountain View, CA, USA), according to the manufacturer's instructions. Cytotoxic effects were measured using the MTS assay (Promega, Madison, WI, USA). For analysis of the apoptotic and pre-apoptotic stages, staining with Annexin V-FITC (BD Biosciences Clontech, Palo Alto, CA, USA) was performed as described (Buytaert et al, 2006; Krysko et al, 2006).

Biotinylation of cell surface proteins

For biotinylation of surface proteins, cells were placed on ice and washed three times with ice-cold PBS-Ca^{2+}-Mg^{2+} (PBS with 0.1 mM $CaCl_2$ and 1 mM $MgCl_2$). Then, 1.25 mg/ml Sulfo-NHS-SS-biotin (Pierce) in biotinylation buffer (10 mM triethanolamine, 2 mM $CaCl_2$, 150 mM NaCl, pH 7.5) was added at 4°C for 30 min of gentle agitation. For control samples (*i.e.* untreated cells), one set of samples was exposed to biotinylation buffer containing biotin (denoted by '+BIO') while the other set was exposed to only biotinylation buffer as a negative control (denoted by '-BIO'). Later, the cells were washed and incubated with the quenching buffer (PBS-Ca^{2+}-Mg^{2+} + 100 mM glycine) for 20 min with gentle agitation at 4°C. The cells were then rinsed twice with PBS, scraped off in ice-cold PBS and pelleted at 2000 rpm and 4°C. The resulting pellets were solubilized in 500 µl lysis buffer (10% glycerol, 1% Triton X-100, 150 mM NaCl, 5 mM EDTA, 50 mM Hepes, pH 7.4 + protease inhibitors) for 40–45 min and the resulting lysates were centrifuged at 14000 x g for 10 min at 4°C. The recovered supernatant was incubated overnight at 4°C with gentle rotation with packed streptavidin-agarose beads (Invitrogen, Carlsbad, CA, USA) in order to separate the biotinylated proteins. The beads were then pelleted by centrifugation and aliquots of supernatants were taken to represent the (unbound)

intracellular proteins. Subsequently, streptavidin-agarose beads were washed three times with washing buffer (10% glycerol, 0.1% Triton X-100, 150 mM NaCl, 20 mM HEPES, pH 7.4). The biotinylated proteins (plasma membrane proteins) were recovered from the beads by heating them at 100°C for 5 min in SDS-PAGE sample buffer. The intracellular protein fractions and plasma membrane protein fractions were then electrophoresed separately (but in parallel) and immunoblotted. The capture of plasma membrane proteins was confirmed by detecting FAS/CD95, ICAM-1 or Na^+/K^+ ATPase in the biotinylated protein fractions. Throughout the figures, 'Plasma membrane proteins' are those in the biotinylated surface protein fraction while 'intracellular proteins' are the unbound, non-biotinylated proteins.

Immunoblotting and conditioned media analysis

Preparation of cell lysates, determination of protein concentration and immunoblotting was done as described (Vantieghem et al, 1998). The bands of proteins on the blots were quantified by using the ImageJ software to determine the relative integrated band density. In some experiments, the 'conditioned' culture media or serum-free media (5–8 ml), as applicable, were collected and concentrated to manageable volumes (200–500 µl) *via* centrifugation (2000 × g for 5 min) using Centricon Plus-20 10-kDa filters (Millipore, Billerica, MA, USA) or Pierce Concentrator 7ml/9K filters (Pierce), according to the manufacturer's instructions. They were then analyzed by immunoblotting.

Estimation of total extracellular secretory protein content

MEF or CT26 cells were treated with indicated doses of Hyp-PDT, washed and recovered for 1 h in serum-free media (5 ml). Later, the 'conditioned' serum-free media were collected and concentrated to manageable

volumes (200 µl) *via* centrifugation (2000 × g for 20 min) using Pierce Concentrator 7ml/9K filters (Pierce), according to the manufacturer's instructions. Simultaneously, lysates were prepared for the cells from which the conditioned media was recovered. This was followed by determination of protein concentration in both concentrated conditioned media and cell lysates *via* BCA protein assay (Pierce) as per the manufacturer's instructions. Within each protein determination it was ensured that the goodness-of-fit of linear regression (r2) for the protein standard curve is no less than 0.99. Total extracellular secretory protein content was calculated by taking a ratio of protein content of concentrated conditioned media and the protein content of the corresponding cell lysates (both in µg/µl), thus accounting for any difference in cell number.

On-cell western analysis for cell surface CRT

For on-cell western analysis of cell surface proteins, the cells were grown in 96-well culture plates to 70–80% confluency, Hyp-PDT treated as indicated, patted dry at various (mentioned) recovery time point, and then placed on ice. The cells were fixed for 20 min with 4% paraformaldehyde at room temperature, washed five times with PBS, and incubated with a blocking solution containing 3% BSA and 5% goat serum for 90 min at room temperature with gentle rocking. The blocking solution was removed and the cells were incubated overnight at 4°C with rabbit anti-human CRT antibody (1:25) (Cell Signaling Technology, Danvers, MA, USA) or rabbit anti-human FAS (N-18) antibody (1:25) (Santa Cruz Biotech, Santa Cruz, CA, USA) in blocking solution. The cells were washed five times with Tween washing solution (PBS + 0.1% Tween-20) and incubated for 1 h at room temperature with an anti-rabbit Alexa Fluor 680 secondary antibody (1:500) (Invitrogen, Carlsbad, CA, USA) in blocking solution (supplemented with 0.2% Tween-20) under low light conditions and with gentle rocking. The plates were washed five times with Tween washing solution, dried, and imaged using the LI-COR Odyssey System. Images were analyzed using Excel (Microsoft Corp., USA) and Prism (GraphPad Software, USA) software.

Fluorescence detection of cell surface CRT and hypericin localization

At suitable recovery time-point following the respective treatments, T24 cells (on a glass slide) were incubated with 1 µM Sytox Green (Invitrogen, Carlsbad, CA, USA) exclusion dye for 15 min. Here, T24 cells permeabilized with 0.1% Saponin were included as positive control for cells with compromised plasma membrane. The principle was that, if a particular cell is permeabilized then its nucleus would stain green and in presence of DAPI counter-stain the overall nucleus of a permeabilized cell would show up as cyan. Following this, the cells were fixed with 4% paraformaldehyde and incubated with 0.1 M glycine (in PBS) followed by incubation with rabbit anti-human CRT antibody (1:25) (Cell Signaling Technology, Danvers, MA, USA) in blocking solution (PBS, 1% BSA, 10% goat serum) (at 4°C for 1 h). They were then washed and incubated with the anti-rabbit IgG antibody conjugated with Alexa fluor 680 (1:500) (Invitrogen, Carlsbad, CA, USA) in blocking solution. The cells were then counterstained with DAPI (1 µg/ml for 10 min) (Invitrogen, Carlsbad, CA, USA) and mounted using Prolong Gold antifade reagent (Invitrogen, Carlsbad, CA, USA). Confocal fluorescence images were acquired at room temperature using a Nikon A1R confocal unit mounted on a Ti2000 inverted microscope controlled by NIS elements acquisition software (Nikon Instruments Inc., Melville, NY, USA).

For experiments on hypericin sub-cellular localization, the CT26 cells were incubated with relevant hypericin concentrations for the indicated durations, counterstained with ER Tracker Blue-White (Invitrogen, Carlsbad, CA, USA), and observed with CellM imaging station (Olympus) consisting of an inverted microscope (IX81; Olympus) followed by images acquisition *via* Cellˆ M software (Olympus). All images were analyzed by using the ImageJ software (W. S. Rasbaud, Image J, NIH, Bethesda, MD, http://rsb.info.nih.gov/ij/).

In vitro phagocytosis assay

In 12-well plates, 2.5×10^5 JAWS II or Mf4/4 cells were labeled with 1 µM Cell tracker Green (Invitrogen, Merelbeke, Belgium) as described previously (Krysko et al, 2006). CT26 and T24 cells harvested 1 h after high Hyp-PDT were washed three times with culture media and co-cultured with JAWS II (CT26) or Mf4/4 cells (T24) for 2 h (at 37°C) at a ratio of 1:5 (JAWSII or Mf4/4:CT26 or T24). Due to the presence of residual hypericin in tumor cells, they did not require additional fluorescent staining for these experiments. Phagocytosis was assessed by analysis of double positive cells (i.e. Cell tracker Green$^+$ and Hypericin$^+$) using a FACSCalibur flow cytometer (Beckton & Dickinson, Mountain View, CA, USA). The percentage of double-positive phagocytes was calculated according to the following formula: 100 × number of double positive cells / (single positive + double positive cells).

In vitro microscopy-based analysis of phagocytic interactions

Phagocytic activity of hu-iDCs was analyzed using a CellM imaging station (Olympus, Hamburg, Germany) consisting of an inverted microscope (IX81; Olympus). T24 cells (incubated on a glass slide) were subjected to high Hyp-PDT dose. One hour later, hu-iDCs labeled with Cell tracker Green at a ratio of 1:20 (hu-iDCs:T24) were added to treated T24 cells for a 4-h co-culture. The cells were washed twice with ice-cold PBS and fixed with 4% paraformaldehyde for 20 min. The cells were then mounted by using Prolong Gold antifade reagent (Invitrogen, Carlsbad, CA, USA) and analyzed under the microscope at room temperature through the Cellˆ M

image acquisition software (Olympus). All images were analyzed by using the ImageJ software (W. S. Rasbaud, Image J, NIH, Bethesda, MD, http://rsb.info.nih.gov/ij/).

LRP1 reconstitution in knock-out (KO) background

Wild-type Chinese hamster ovary cells (CHO K1) and derived LRP1-deficient CHO cells (CHO 13-5-1) were provided by Dr. D. FitzGerald (National Institute of Health, Bethesda, Maryland) (FitzGerald et al, 1995). Stable restoration of LRP1 function in CHO 13-5-1 was achieved by transfection of a full-length murine LRP1 cDNA cloned in a pcDNA3 plasmid vector (Invitrogen) using FuGENE (Promega) (Smeijers et al, 2002). The LRP1-restored CHO 13-5-1 cell line was cloned by G418 selection (600 µg/ml) (Invitrogen) and limiting dilution.

References:

Buytaert E, Callewaert G, Hendrickx N, Scorrano L, Hartmann D, Missiaen L, Vandenheede JR, Heirman I, Grooten J, Agostinis P (2006) Role of endoplasmic reticulum depletion and multidomain proapoptotic BAX and BAK proteins in shaping cell death after hypericin-mediated photodynamic therapy. *FASEB J* **20**(6)**:** 756-758

FitzGerald DJ, Fryling CM, Zdanovsky A, Saelinger CB, Kounnas M, Winkles JA, Strickland D, Leppla S (1995) Pseudomonas exotoxin-mediated selection yields cells with altered expression of low-density lipoprotein receptor-related protein. *J Cell Biol* **129**(6)**:** 1533-1541

Krysko DV, Denecker G, Festjens N, Gabriels S, Parthoens E, D'Herde K, Vandenabeele P (2006) Macrophages use different internalization mechanisms to clear apoptotic and necrotic cells. *Cell Death Differ* **13**(12)**:** 2011-2022

Smeijers L, Willems S, Lauwers A, Thiry E, van Leuven F, Roebroek AJ (2002) Functional expression of murine LRP1 requires correction of Lrp1 cDNA sequences. *Biochim Biophys Acta* **1577**(1)**:** 155-158

Vantieghem A, Assefa Z, Vandenabeele P, Declercq W, Courtois S, Vandenheede JR, Merlevede W, de Witte P, Agostinis P (1998) Hypericin-induced photosensitization of HeLa cells leads to apoptosis or necrosis. Involvement of cytochrome c and procaspase-3 activation in the mechanism of apoptosis. *FEBS Lett* **440**(1-2)**:** 19-24

Supplemental Table

A novel pathway combining calreticulin exposure and ATP secretion in immunogenic cancer cell death

Abhishek D. Garg, Dmitri V. Krysko, Tom Verfaillie, Agnieszka Kaczmarek, Gabriela B. Ferreira, Thierry Marysael, Noemi Rubio, Malgorzata Firczuk, Christine Michiels, Chantal Mathieu, Anton J. M. Roebroek, Wim Annaert, Jakub Golab, Peter de Witte, Peter Vandenabeele and Patrizia Agostinis

Table S1. Sequences of shRNAs targeted against murine LRP1, PI3K p110α, PERK and Caspase-8. CT26 cells were stably transfected with shRNAs against the murine mRNAs listed above. Each mRNA was targeted with three different shRNA constructs. The sequences and further remarks about each shRNA (if any) is mentioned.

shRNA	shRNA sequences	Remarks
LRP1 shRNA	**shRNA 1** – CCGGGCTGAACACATTCTTTGGTAACTC GAGTTACCAAAGAATGTGTTCAGCTTTTTG (Clone ID NM_008512.1-14655s1c1)	Gave the best knock-down (Fig S13, A). Used for further experiments.
	shRNA 2 –CCGGCCTACCTACAAGATGTATGAACT CGAGTTCATACATCTTGTAGGTAGGTTTTTG (Clone ID NM_008512.1-13855s1c1)	-
	shRNA 3 – CCGGGCTGAACACATTCTTTGGTAACT CGAGTTACCAAAGAATGTGTTCAGCTTTTTG (Clone ID NM_008512.2-14674s21c1)	Cells transfected with this shRNA did not survive.
PI3K p110α shRNA	**shRNA 1** – CCGGGCCGATTGATAGCTTCACCATCT CGAGATGGTGAAGCTATCAATCGGCTTTTT (Clone ID NM_008839.1-891s1c1)	-
	shRNA 2 – CCGGGCAACCTTTATCTTGGGAATTCTCGA GAATTCCCAAGATAAAGGTTGCTTTTT (Clone ID NM_008839.1-2719s1c1)	Cells transfected with this shRNA did not survive.
	shRNA 3 – CCGGCCAGATGTACTGCTTAGTAAAC TCGAGTTTACTAAGCAGTACATCTGGTTTTT (Clone ID NM_008839.1-1743s1c1)	Gave the best knock-down (Fig S9, C). Used for further experiments.
PERK shRNA	**shRNA 1** – CCGGGCCACTTTGAACTTCGGTATACTCG AGTATACCGAAGTTCAAAGTGGCTTTTT (Clone ID NM_010121.1-964s1c1)	-
	shRNA 2 – CCGGCCATGAGTTCATCTGGAACAACTC GAGTTGTTCCAGATGAACTCATGGTTTTT (Clone ID NM_010121.1-3466s1c1)	-
	shRNA 3 – CCGGCCTCTACTGTTCACTCAGAAAC TCGAGTTTCTGAGTGAACAGTAGAGGTTTTT (Clone ID NM_010121.1-3303s1c1)	Gave the best knock-down (Fig S10, A). Used for further experiments.
Caspase-8 shRNA	**shRNA 1** – CCGGCCTCCATCTATGACCTGACATCTC GAGATGTCAGGTCATAGATGGAGGTTTTT (Clone ID NM_009812.1-1271s1c1)	Gave the best knock-down (Fig S11, A). Used for further experiments.
	shRNA 2 – CCGGGTGTGGATGAGTCTAATTTATCTC GAGATAAATTAGACTCATCCACACTTTTT (Clone ID NM_009812.1-1762s1c1)	-
	shRNA 3 – CCGGCCTCCATCTATGACCTGACATCTC GAGATGTCAGGTCATAGATGGAGGTTTTT (Clone ID NM_009812.1-1271s1c1)	-